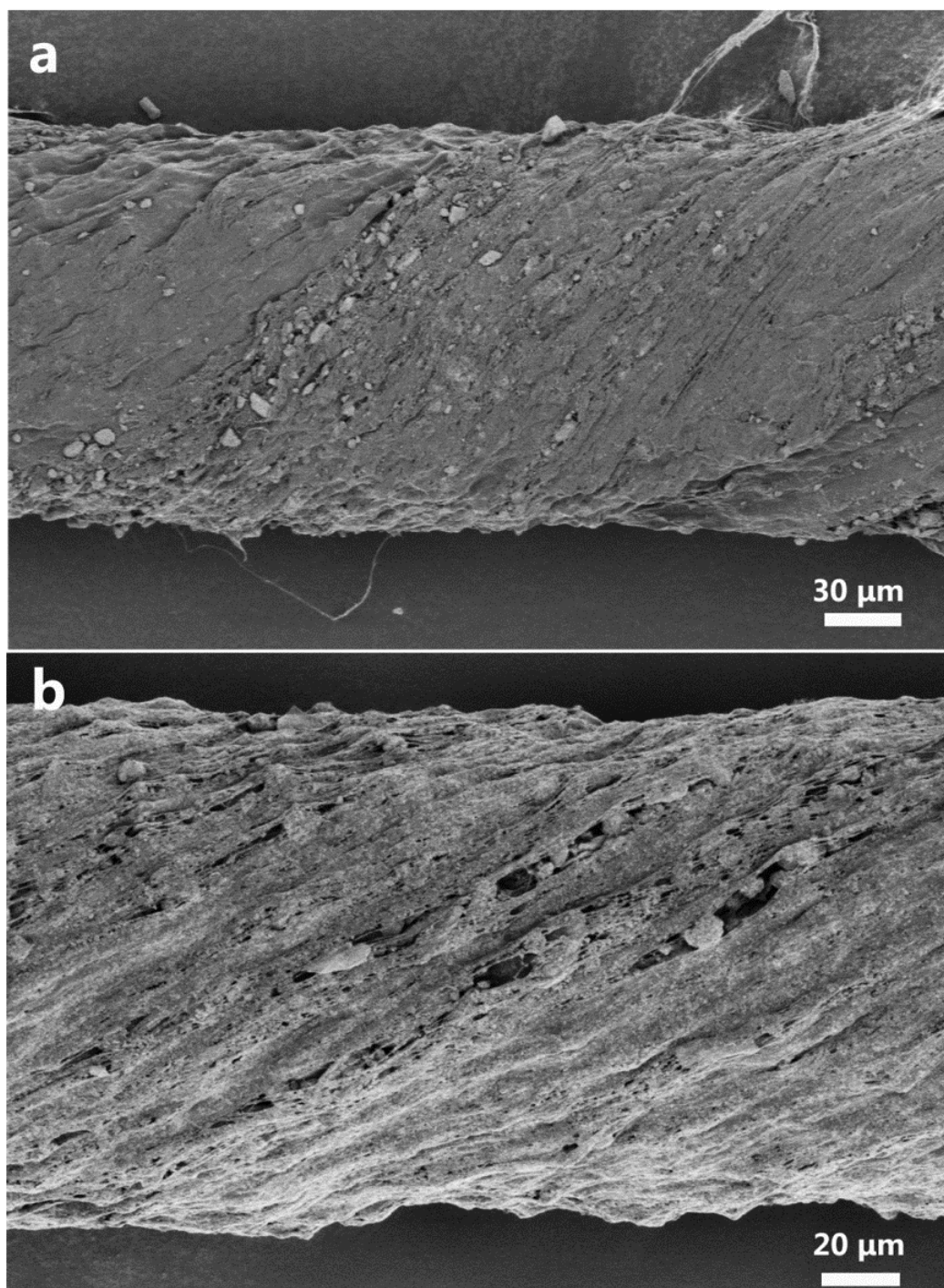
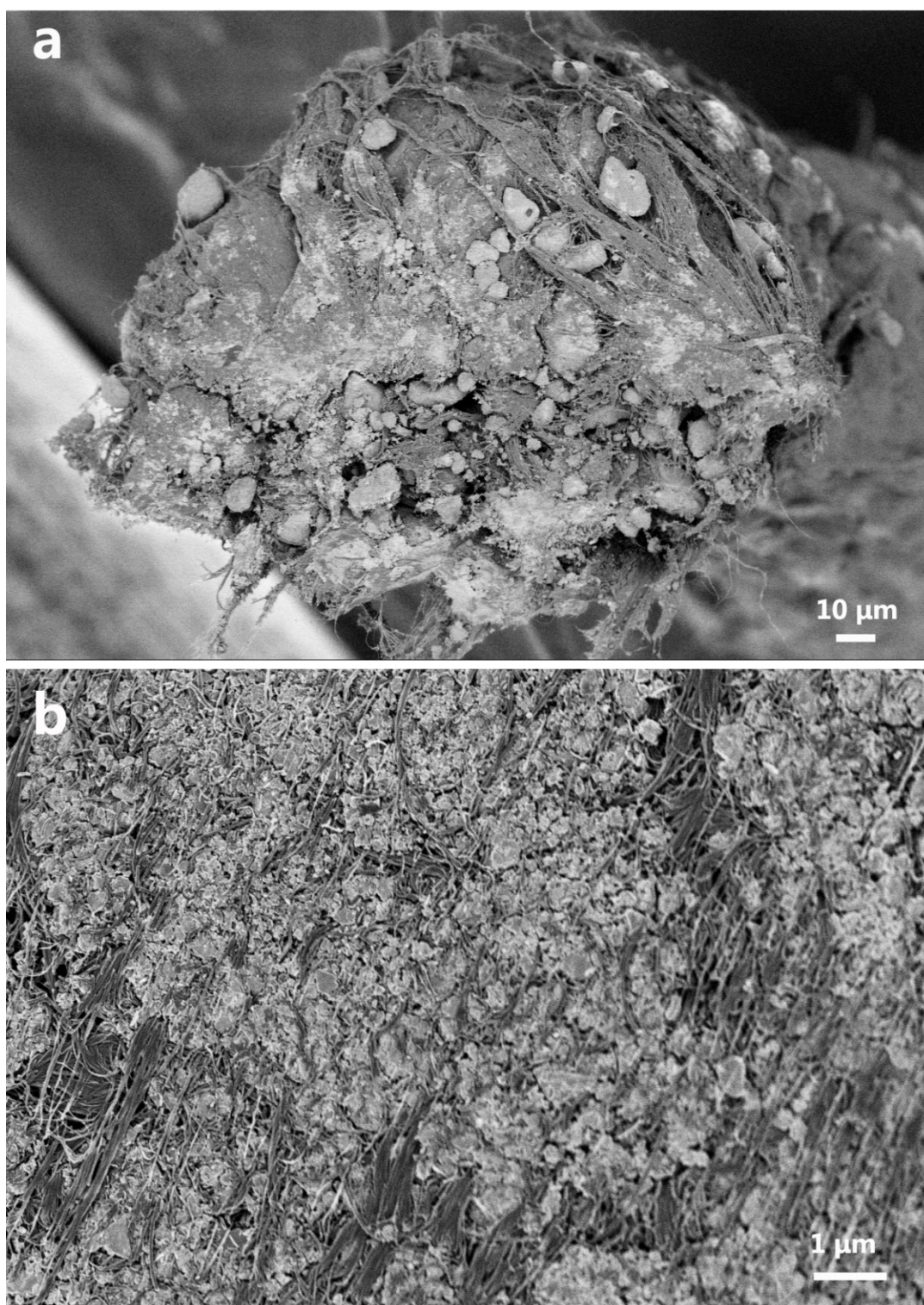


## Supporting Information

**Video S1:** The highly stretchable property of the fiber-shaped lithium ion battery.



**Figure S1. a and b.** SEM images of MWCNT/LiMn<sub>2</sub>O<sub>4</sub> and MWCNT/Li<sub>4</sub>Ti<sub>5</sub>O<sub>12</sub> composite fibers, respectively.



**Figure S2. a and b.** Cross-sectional SEM images of an MWCNT/LiMn<sub>2</sub>O<sub>4</sub> composite fiber at low and high magnifications, respectively.



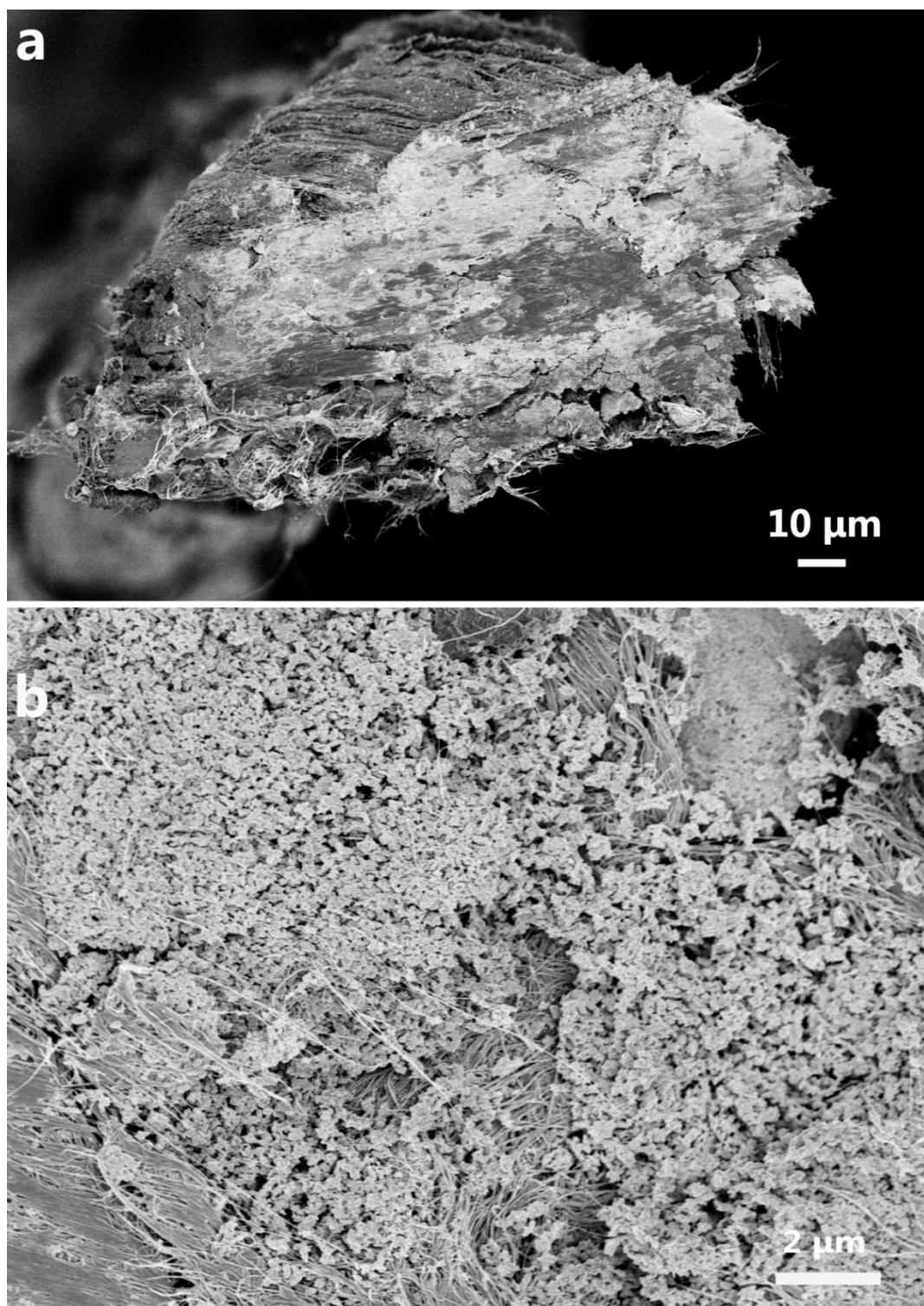


**Figure S3. a and b.** Cross-sectional SEM images of an MWCNT/Li<sub>4</sub>Ti<sub>5</sub>O<sub>12</sub> composite fiber at low and high magnifications, respectively.

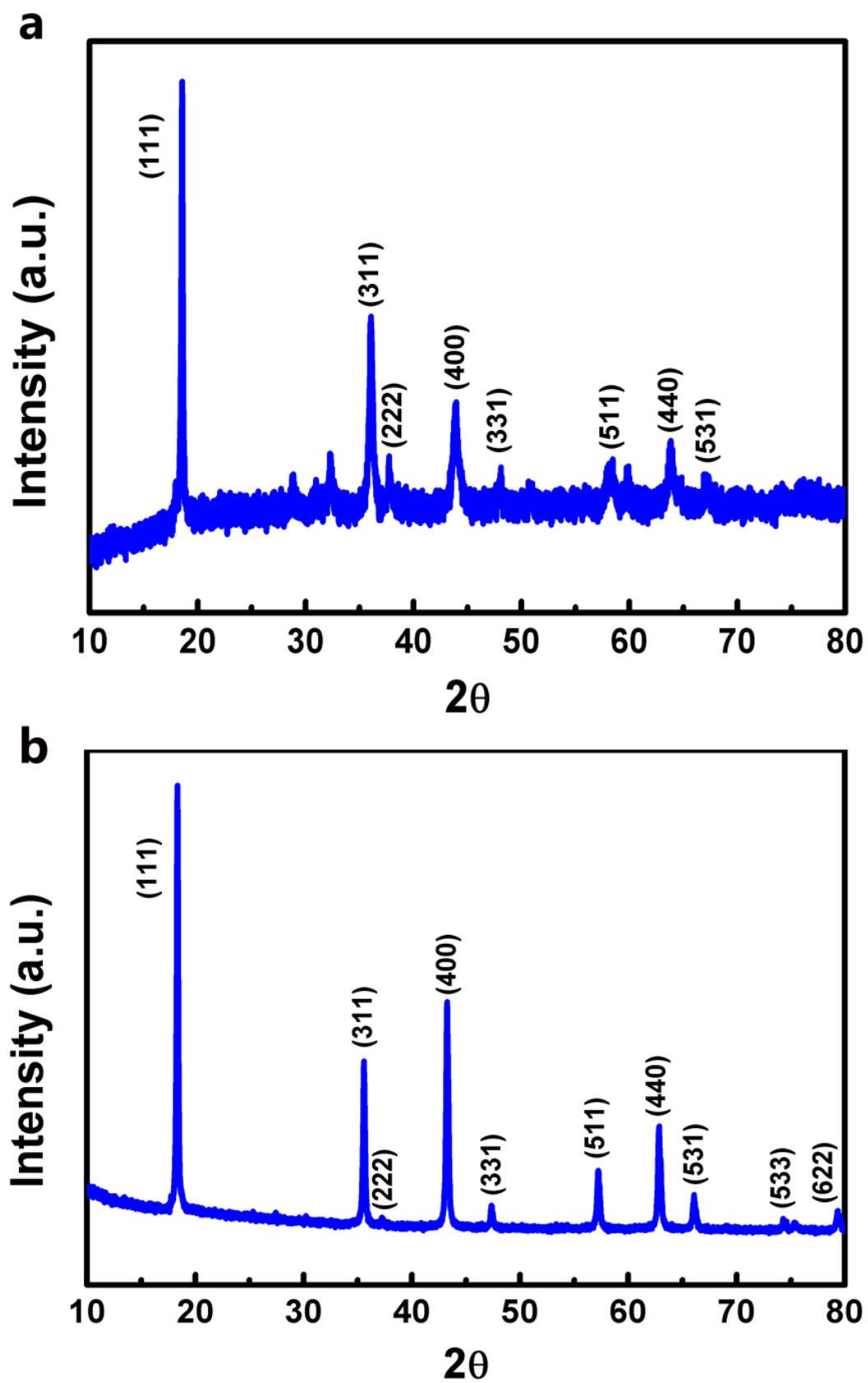


**Figure S4. a and b.** X-ray diffraction patterns of pure  $\text{LiMn}_2\text{O}_4$  and  $\text{Li}_4\text{Ti}_5\text{O}_{12}$  particles, respectively.



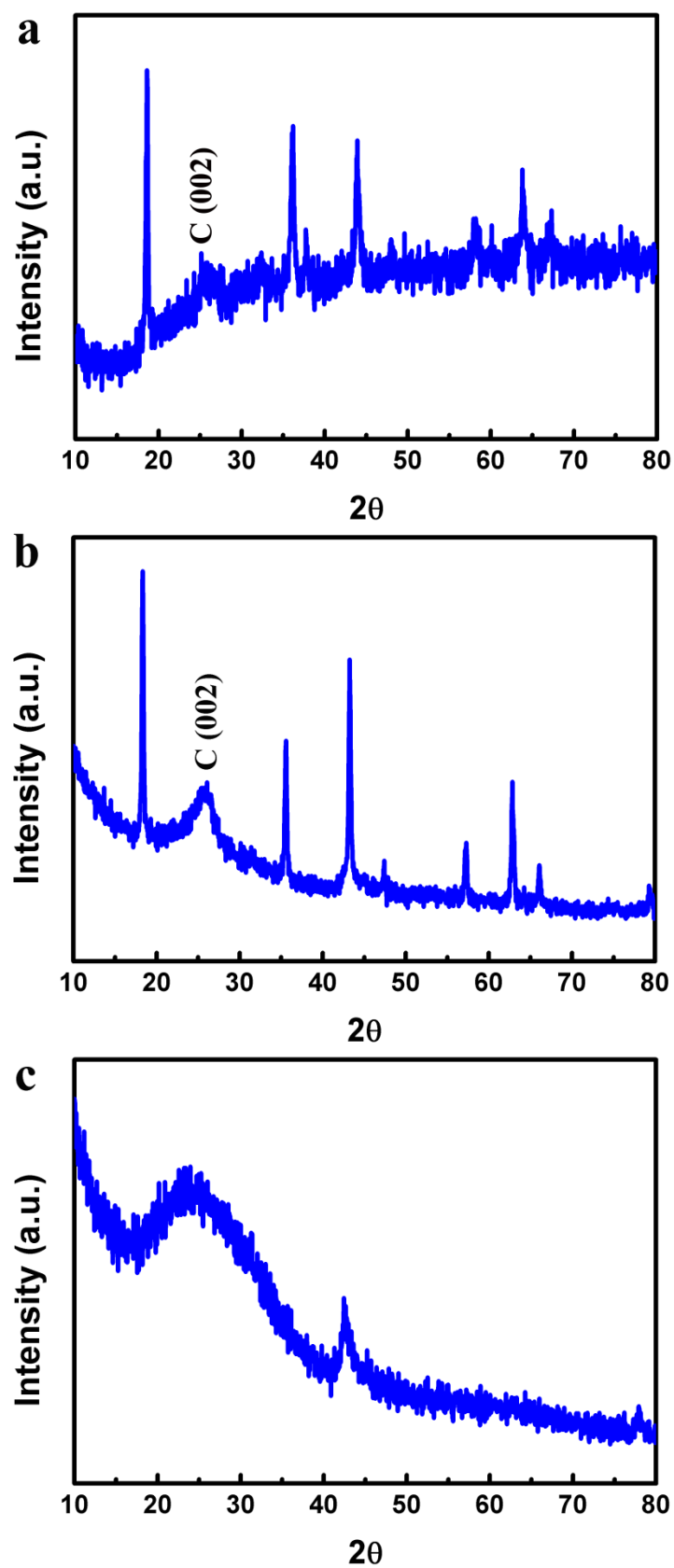


**Figure S5. a, b and c.** X-ray diffraction patterns of MWCNT/LiMn<sub>2</sub>O<sub>4</sub> composite fiber, MWCNT/Li<sub>4</sub>Ti<sub>5</sub>O<sub>12</sub> composite fiber and pure MWCNT fiber, respectively.

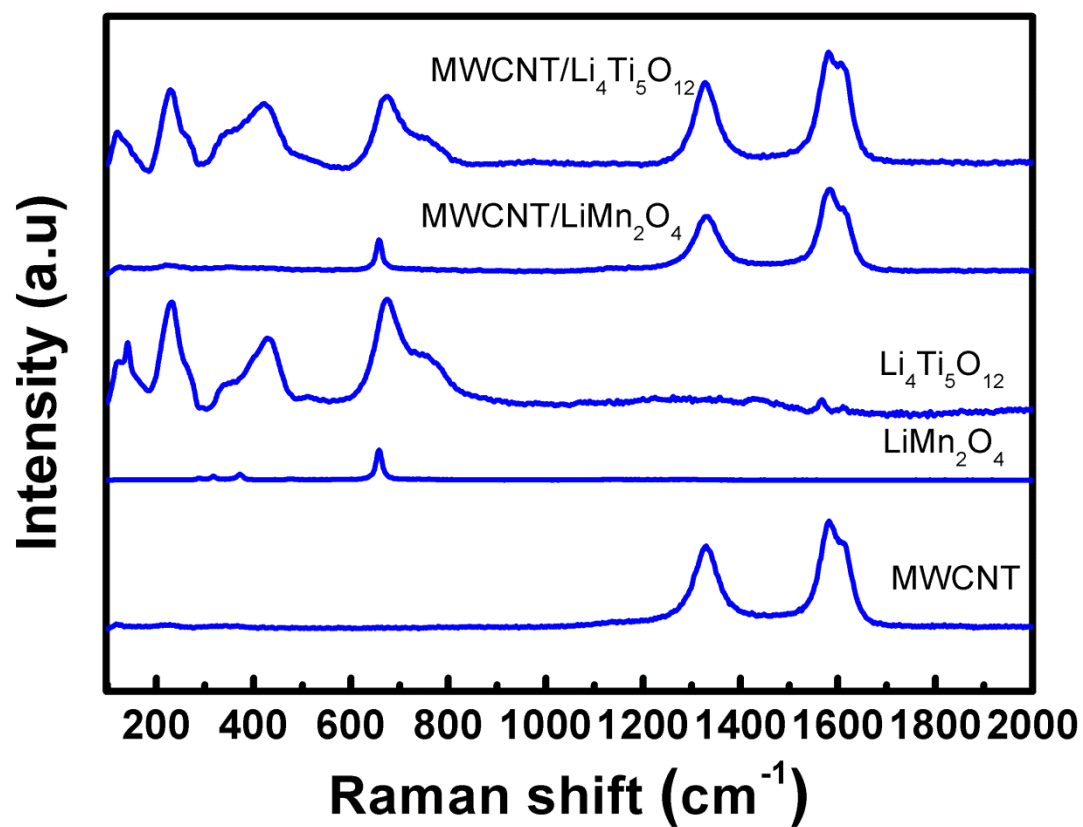


**Figure S6.** Raman spectra of MWCNT, LiMn<sub>2</sub>O<sub>4</sub>, Li<sub>4</sub>Ti<sub>5</sub>O<sub>12</sub>, MWCNT/LiMn<sub>2</sub>O<sub>4</sub> and MWCNT/Li<sub>4</sub>Ti<sub>5</sub>O<sub>12</sub> composite fibers.

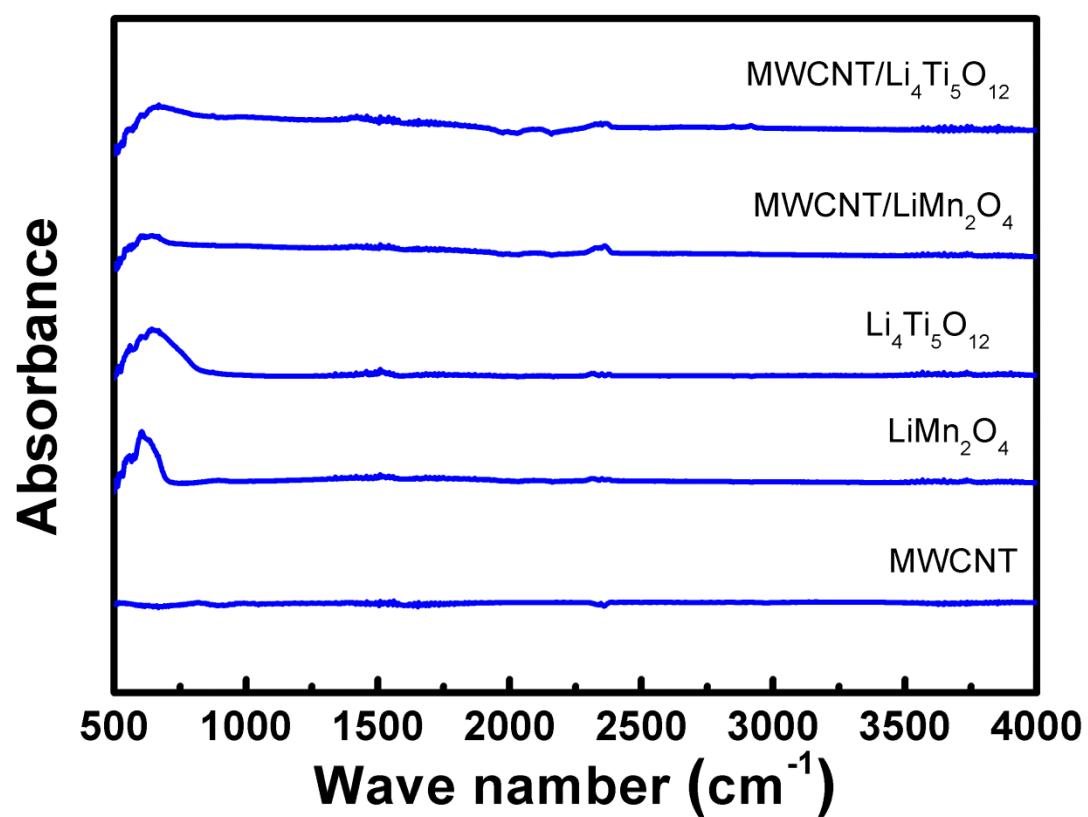


**Figure S7.** FTIR spectra of MWCNT, LiMn<sub>2</sub>O<sub>4</sub>, Li<sub>4</sub>Ti<sub>5</sub>O<sub>12</sub>, MWCNT/LiMn<sub>2</sub>O<sub>4</sub> and MWCNT/Li<sub>4</sub>Ti<sub>5</sub>O<sub>12</sub> composite fibers.



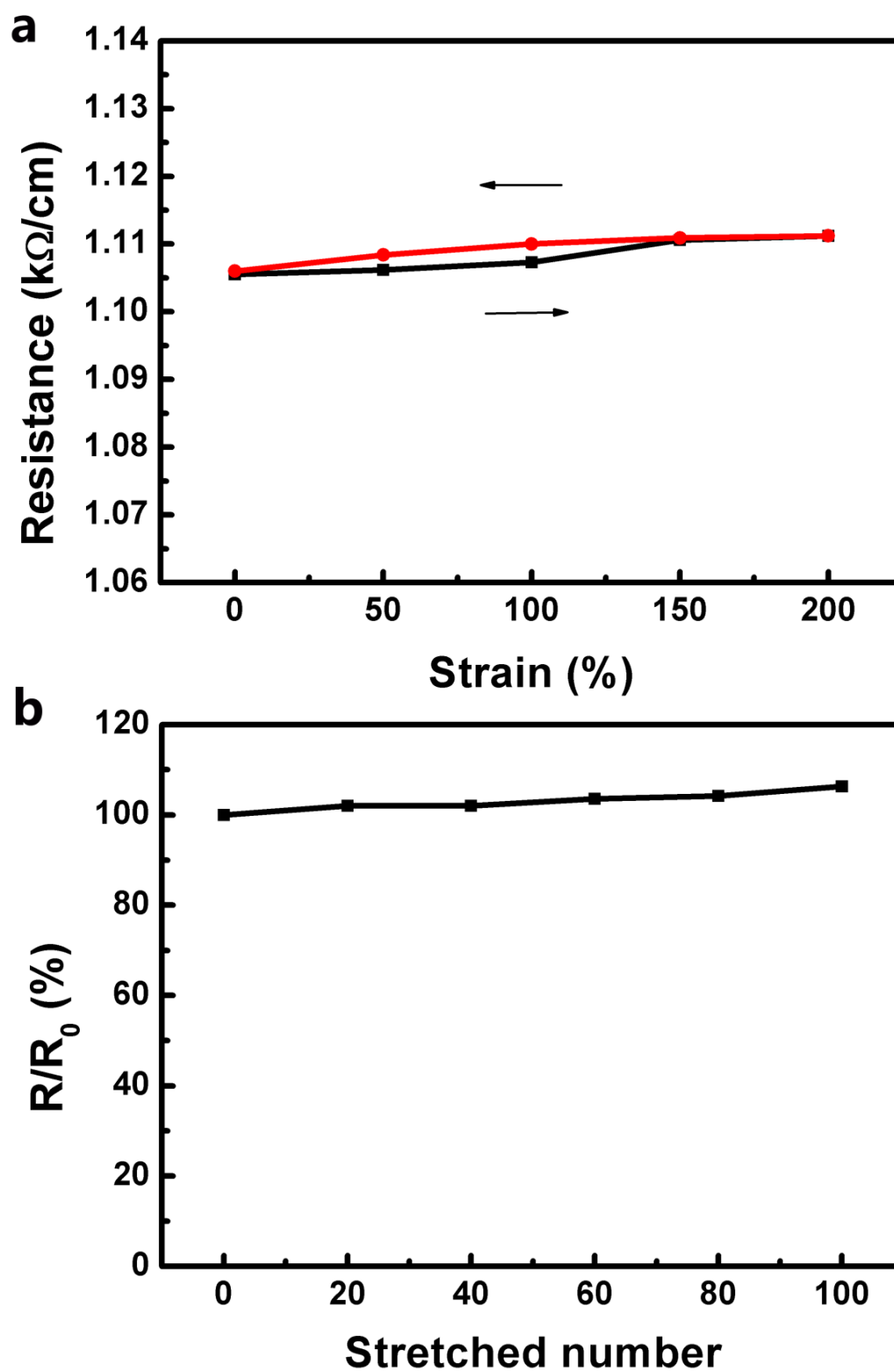


**Figure S8.** **a.** Changes of resistances for the positive electrode during the stretching and releasing process with a strain of 200%. **b.** Dependence of resistance on stretched number (at a strain of 200%).  $R_0$  and  $R$  correspond to resistances before and after stretching, respectively.

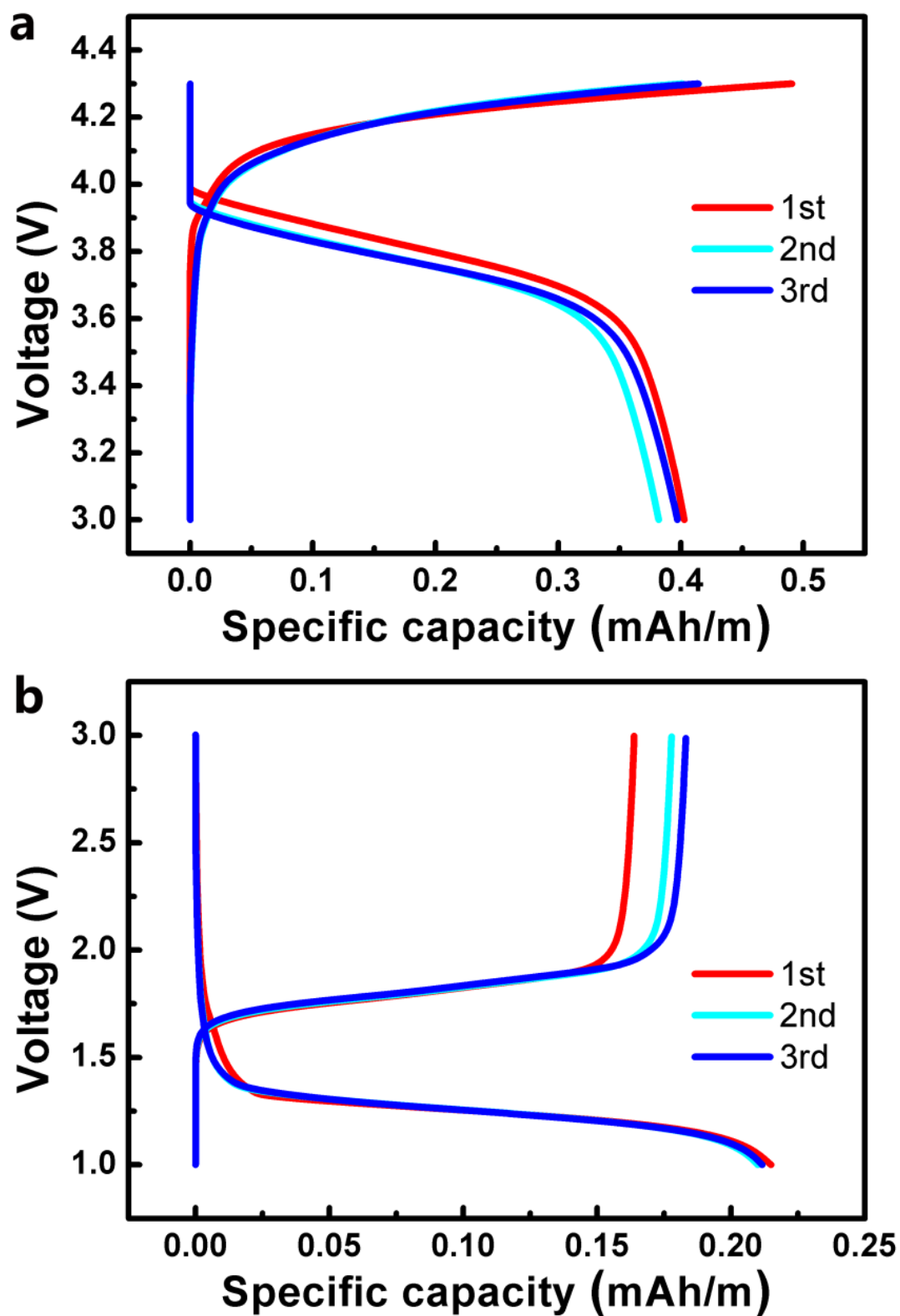


**Figure S9. a and b.** Charge and discharge profiles of positive (MWCNT/LiMn<sub>2</sub>O<sub>4</sub> composite fiber) and negative (MWCNT/Li<sub>4</sub>Ti<sub>5</sub>O<sub>12</sub> composite fiber) electrodes in half cells with lithium as the counter electrode, respectively.

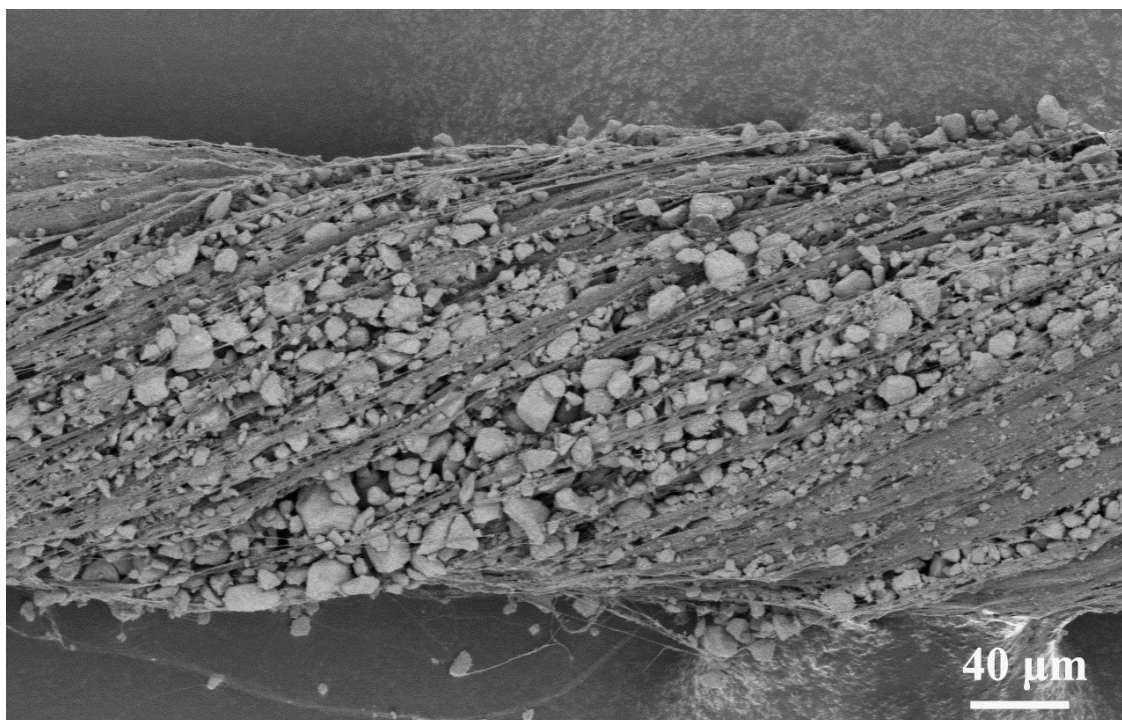


**Figure S10.** SEM image of the MWCNT/LiMn<sub>2</sub>O<sub>4</sub> composite fiber (weight percentage of 87% for the LiMn<sub>2</sub>O<sub>4</sub>).



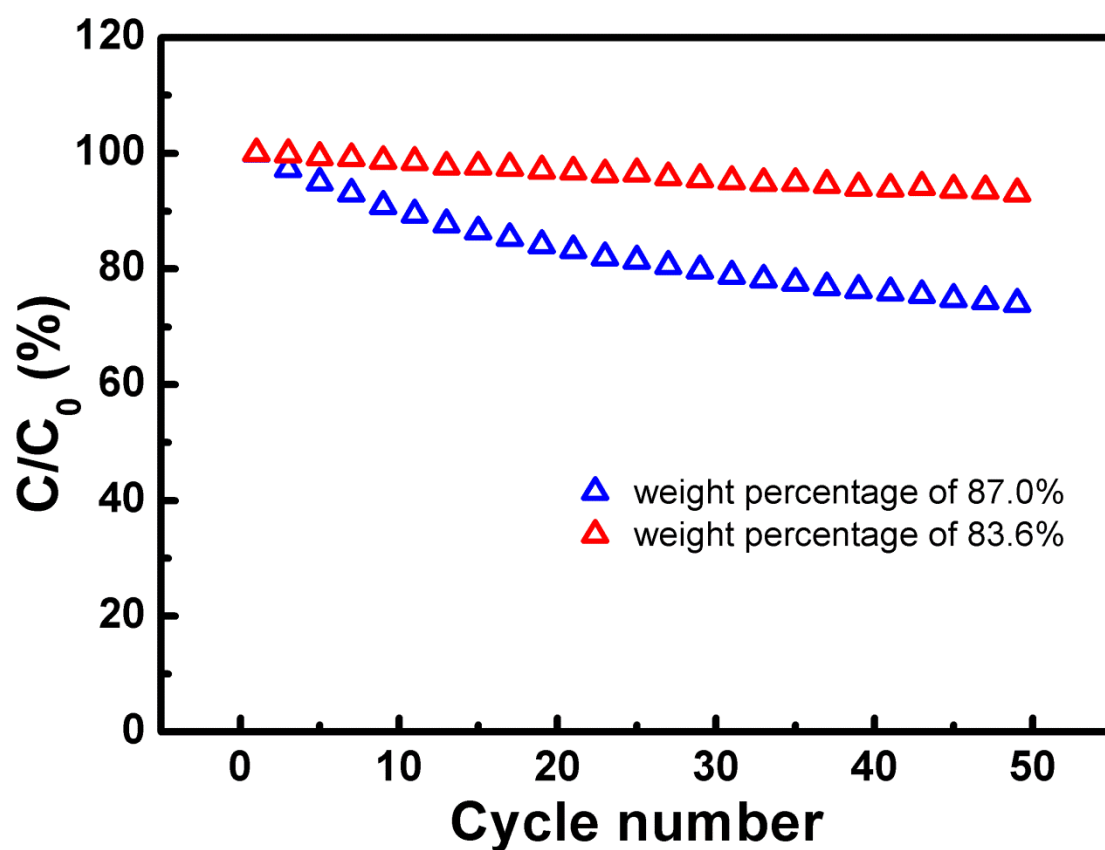


**Figure S11.** Dependence of specific capacity of positive electrode (MWCNT/LiMn<sub>2</sub>O<sub>4</sub> composite fiber) in half cells on cycle number.  $C_0$  and  $C$  correspond to the specific capacities at the first and following cycle, respectively.

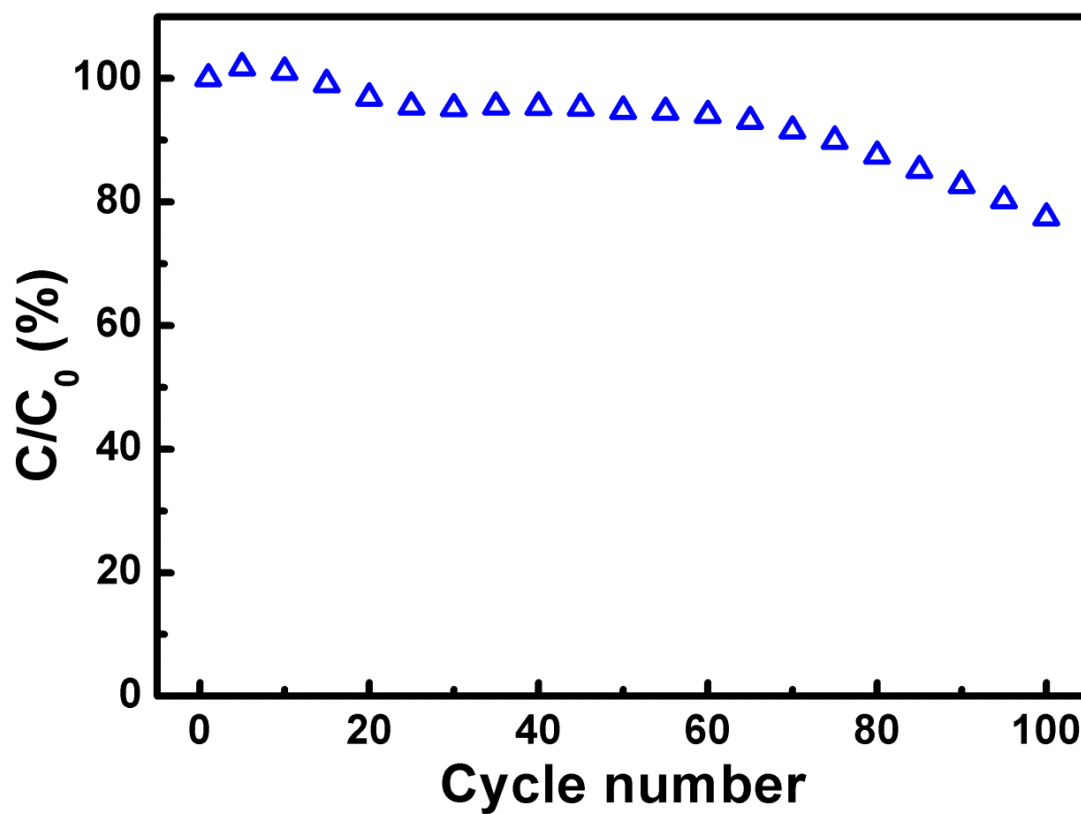


**Figure S12.** Dependence of specific capacity of a fiber-shaped battery on cycle number.  $C_0$  and  $C$  correspond to the specific capacity at the first and following cycle, respectively.

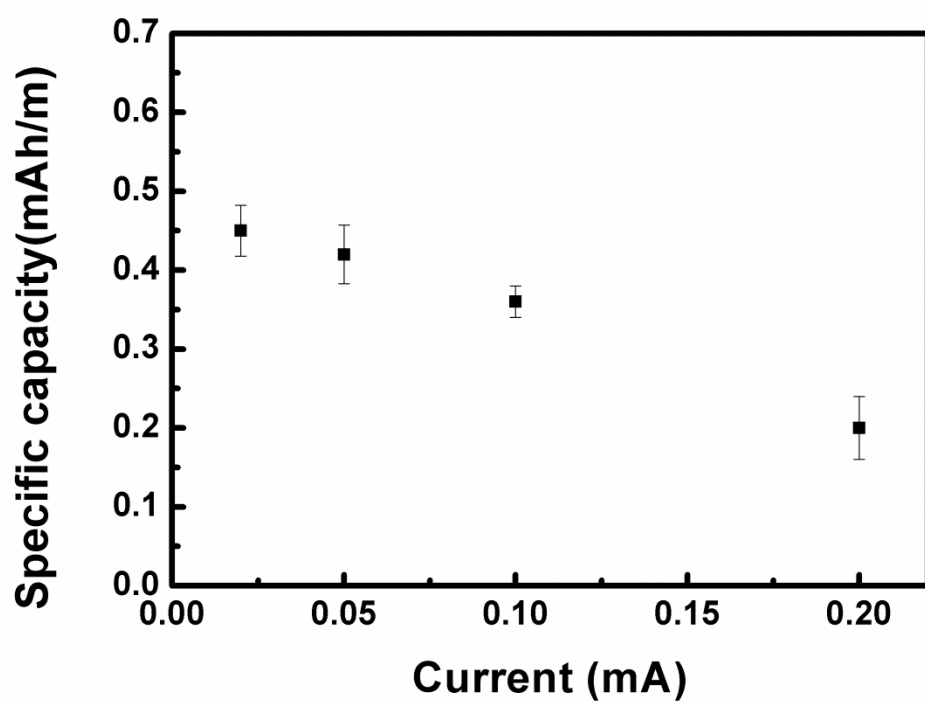


**Figure S13.** Dependence of specific capacity of a fiber-shaped battery on current.



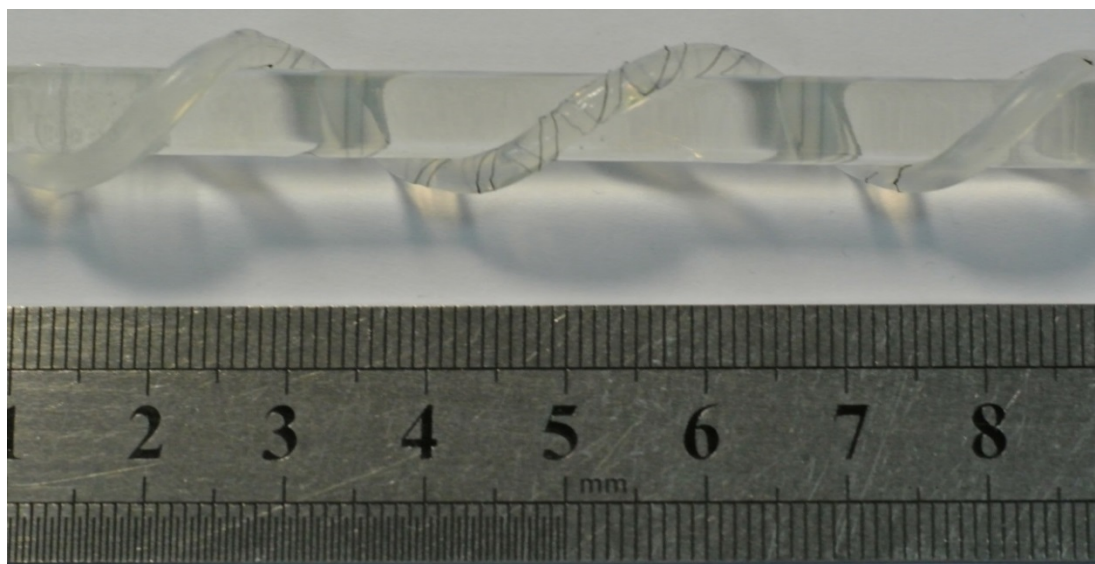


**Figure S14.** Photograph of a stretchable fiber-shaped battery being wound on a glass rod.

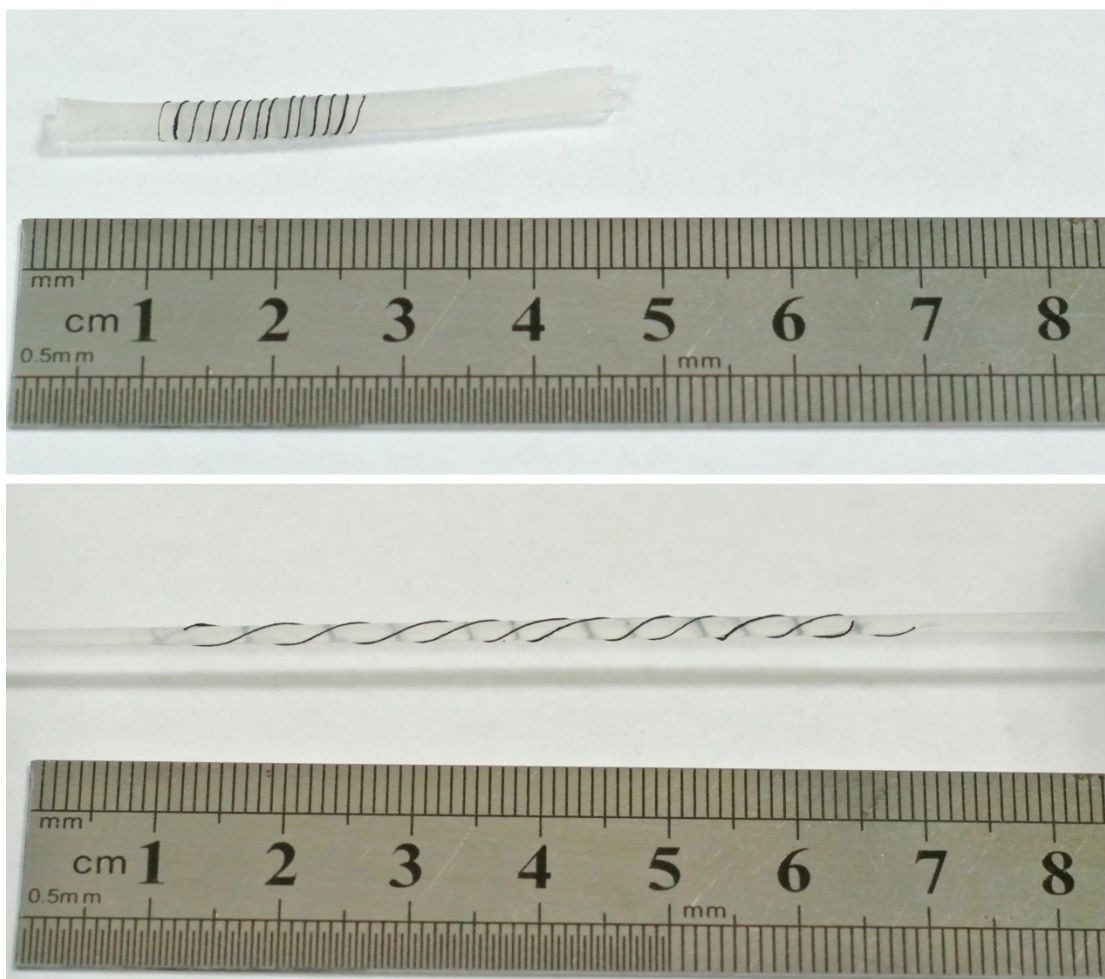


**Figure S15.** Photographs of a stretchable fiber-shaped battery with a strain over 200%.

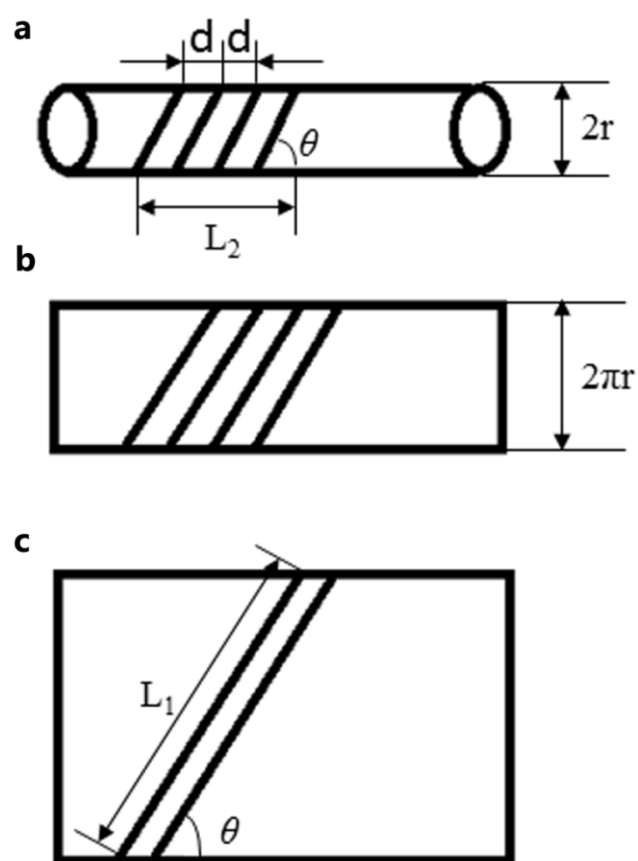


**Figure S16.** Schematic illustration to the stretchability of a fiber-shaped lithium-ion battery based on the twist structure.



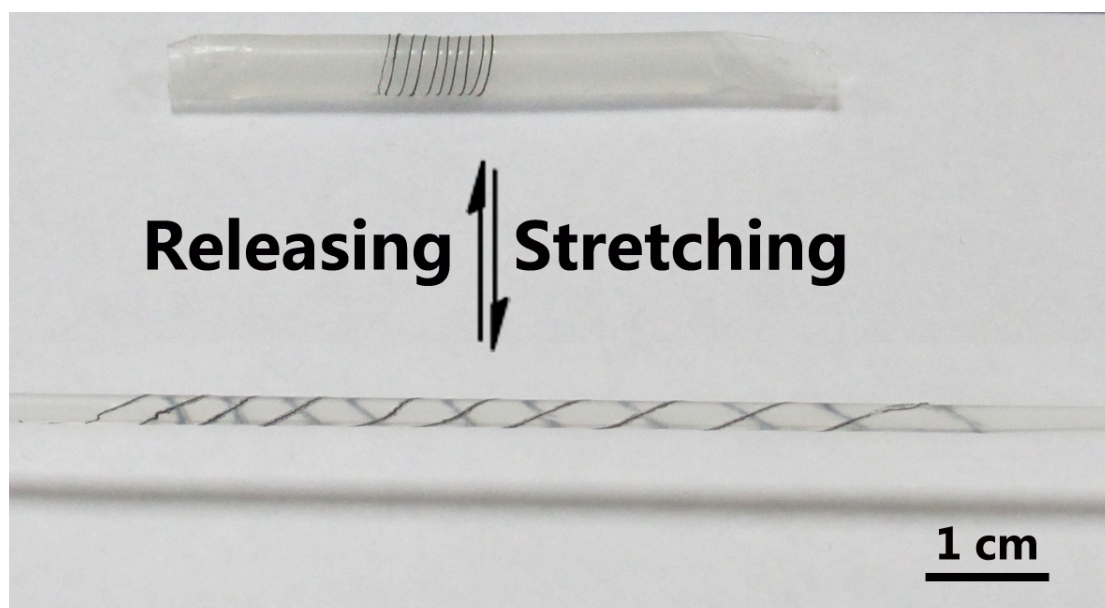


**Figure S17.** Photograph of a stretchable fiber-shaped battery with a strain of 600%.

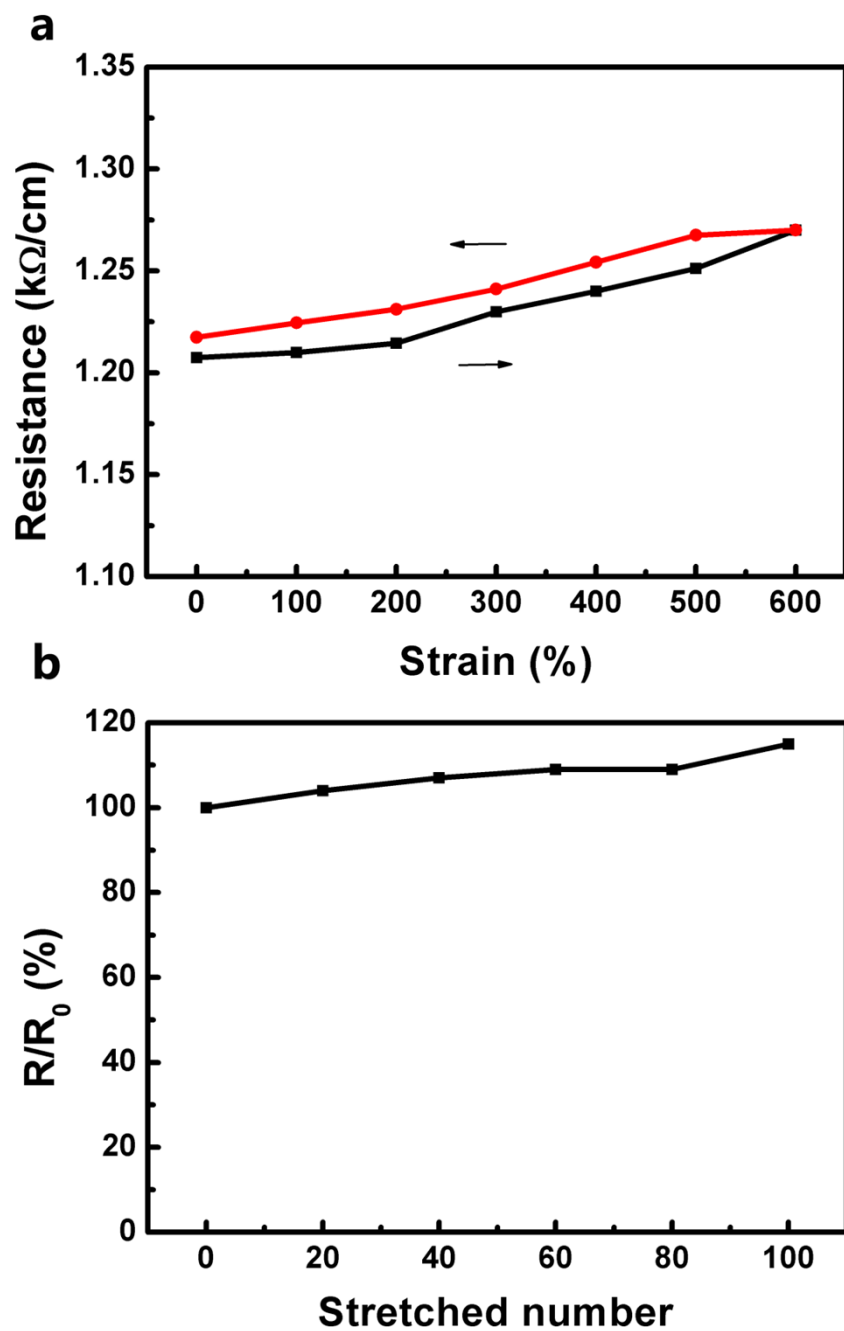


**Figure S18. a.** Changes of resistances for the positive electrode during the stretching and releasing process with a strain of 600%. **b.** Dependence of resistance on stretched number at the strain of 600%.  $R_0$  and  $R$  correspond to resistances before and after stretching, respectively.